Article

Not peer-reviewed version

Green Synthesis of Silver Nanoparticles Using *Fructus mori* Juice: Characterization and Research of Antioxidant and Antibacterial Properties

Fangzheng Liu , Jisheng Li * , Binbin Wang , Wei Fan , Manli Jia , Na Li , Yongxue Song , Chuanjing An , Xiaoxuan Liu , Xiaoqing Jie

Posted Date: 14 November 2023

doi: 10.20944/preprints202311.0868.v1

Keywords: silver nanoparticles; Fructus mori; green synthesis; antibacterial properties; antioxidant activity

Article

Green Synthesis of Silver Nanoparticles Using *Fructus mori* Juice: Characterization and Research of Antioxidant and Antibacterial Properties

Fangzheng Liu [1,2,3], Jisheng Li [1,3,4,*], Binbin Wang [1,3,4], Wei Fan [1,3,4], Manli Jia [1,3,4], Na Li [1,3,4], Yongxue Song [1,3,4], Chuanjing An [1,3,4], Xiaoxuan Liu [1,2,3] and Xiaoqing Jie [1,3,4]

[1] Institute of Sericulture, Chengde Medical University, Chengde 067000, Hebei, China
[2] Department of Biomedical Engineering, Chengde Medical University, Chengde 067000, Hebei, China
[3] Applied Technology R&D Center for Special Sericulture of Hebei Province Universities, Chengde 067000, Hebei, China
[4] Department of Biological Science and Technology, Chengde Medical University, Chengde 067000, Hebei, China
* Correspondence: jshlee@cdmc.edu.cn (J. L.)

Abstract: Novel antibacterial silver nanomaterials have become promising substitutes for traditional antibiotics, because pathogens do not develop resistance to them. However, it is necessary to produce silver nanoparticles with appropriate size and better performance through a green and simple synthesis process. In the present study, *Fructus mori*-composite silver nanoparticles (M-AgNPs) were greenly synthesized using medicinal plant mulberry fruits (*Fructus mori*), with silver nitrate ($AgNO_3$) as a precursor. UV-Vis spectroscopy and X-ray diffraction (XRD) indicated the formation of silver nanoparticles with face centered cubic structure. Fourier transform infrared (FTIR) spectroscopy confirmed the reducing and capping effects of mulberry fruits' active components (polyphenols, flavonoids, etc.) on M-AgNPs. The reaction parameters including temperature, time, pH, and concentration of $AgNO_3$ were gradually optimized. The particle size and morphology of M-AgNPs were measured by dynamic light scattering (DLS) and transmission electron microscopy (TEM) techniques. The minimum particle size of M-AgNPs was about 30 nm, and they were approximately spherical and equably distributed. The excellent stability of M-AgNPs ensured that no agglomeration occurred for up to 60 days. The antioxidant activity of M-AgNPs was evaluated by 1,1-diphenyl-2-trinitrophenylhydrazine (DPPH) assay, and the DPPH radical clearance rate of M-AgNPs was up to about 79%. Greenly synthesized M-AgNPs exhibited better antibacterial activity than chemically synthesized commercial silver nanoparticles (C-AgNPs), due to the active molecules attached to their surfaces. The inhibition zone diameters of M-AgNPs against P.aeruginosa, E.coli and S.aureus were 13.9±0.4、12.2±0.3、12.8±0.7 mm, respectively. Such greenly synthesized AgNPs from medicinal plants have good prospects in the field of biomedicine.

Keywords: silver nanoparticles; *Fructus mori*; green synthesis; antibacterial properties; antioxidant activity

1. Introduction

With the extensive use of antibiotics, pathogens have developed multidrug resistance, which brings great burden to the medical system and patients [1]. The World Health Organization has listed bacterial resistance as one of the three most important public health threats in the 21st century, and medical researchers strive to develop innovative strategies to combat these drug-resistant pathogens. Silver nanoparticles (AgNPs) with unique physical and chemical properties have gradually become a research hotspot in the field of biomedicine because of their antibiosis, antioxidant, anticancer, drug delivery, medical implantation, biosensors and other functions [2–4]. Optimistically, pathogens do not easily develop resistance to silver nanoparticles [5], because the antibacterial mechanism of AgNPs is multi-way [6], including functional protein denaturation, DNA damage, ribosome

 doi:10.20944/preprints202311.0868.v1

degradation, respiratory chain function destruction, and oxidative stress [7]. Consequently, AgNPs can be used as promising substitutes for traditional antibiotics.

AgNPs can be produced by many methods, for example chemical methods (chemical reduction, vapor deposition, photochemical reduction, electrochemical reduction, etc.) and physical methods (mechanical grinding, laser cautery, evaporation and condensation, etc.) [8,9]. However, at present, the key of this research is to produce AgNPs with appropriate size and properties by an environmentally friendly and simple preparation process. Compared with traditional chemical and physical synthesis methods, biological preparation methods avoid the problems of harmful reagents, complex and expensive equipment [10]. The biosynthesis of AgNPs uses plants, bacteria and fungi as raw materials [11]. Among them, plant reduction is the most popular way due to advantages of low cost, easy access, safety, environmental friendliness, and rapid synthesis. Furthermore, active compounds in plants, such as flavonoids, phenolic acids, reducing sugar, alkaloids, and terpenoids, can play the dual roles as reducing agent and capping agent in the process of synthesizing AgNPs [12], especially for medical plants rich in active substances [13].

Mulberry is a folk medical plant, which is widely distributed in many provinces in China and has a history of more than 5,000 years [14]. The mulberry fruit (*Fructus mori*) contains many active ingredients, such as flavonoids (anthocyanins, quercetin, rutin, etc.), phenolic acids (chlorogenic acid, gallic acid, etc.), sugars (glucose, galactose, mannose, etc.), amino acids (glutamic acid, aspartic acid, etc.), vitamins (vitamin A, vitamin C, etc.) and minerals (potassium, calcium, zinc, etc.) [15–17]. Modern medical research has found that mulberry fruit has good antioxidation, anti-inflammatory, anticancer and immunomodulatory effects, as well as preventive and improving effects on diabetes and cardiovascular and cerebrovascular diseases [18–22]. This research expects to combine "green synthesis of AgNPs" with "diversified utilization of mulberry".

Our previous work shows that "AnShen" is an excellent mulberry fruit variety, rich in pharmacological components [23]. For example, the contents of total flavonoids and total phenols are 26.5 and 25.2 mg/g, respectively, much higher than other varieties [14]. These potential reducing and capping components are beneficial for synthesizing AgNPs. Therefore, in this study, the fruit juice of "AnShen" was used as the raw material to synthesize *Fructus mori*-composite silver nanoparticles (M-AgNPs). Through optimizing parameters of the synthesis process, spherical and equably distributed M-AgNPs were obtained, with a particle size of about 30 nm. The antioxidant activity of M-AgNPs was evaluated by the DPPH method. Common drug-resistant pathogens like *S.aureus*, *E.coli* and *P.aeruginosa* were taken as the research objects to investigate the antibacterial properties of M-AgNPs, and compared with commercial silver nanoparticles (C-AgNPs) synthesized by chemical method. The results show that the biosynthetic M-AgNPs has stronger antibacterial activity than the chemically synthesized C-AgNPs. Our study could expand knowledge in the green biosynthesis and future bio-applications of silver nanoparticles.

2. Materials and Methods

2.1. Materials

The mulberry fruits were collected from Sericulture Science Park of Chengde Medical University (longitude: 117.96, latitude: 41.03). The standard solution of silver nitrate ($AgNO_3$), sodium chloride (NaCl, AR) and sodium hydroxide (NaOH, AR) were purchased from Aladdin Company (China). 2,6-di-tert-butyl-p-cresol (BHT, AR), 1,1-diphenyl-2-trinitrophenylhydrazine (DPPH, BR) were purchased from Macklin Company (China). Tryptone, yeast extract powder and agar powder were purchased from Beijing Aoboxing Company (China), all of which are biological reagents. Commercial silver nanoparticles (purity > 99%) were purchased from ZhongKeKeYou Company (China). *S.aureus* [CMCC(B)26003], *E.coli* [CMCC(B)44102] and *P.aeruginosa* [CMCC(B)10104] were prepared by China Medical Culture Collection (CMCC).

 doi:10.20944/preprints202311.0868.v1

2.2. Preparation of mulberry fruit juice

Freshly picked mulberry fruits were washed three times with ultrapure water before the juice was extracted using a juicer (Joyoung, Z8-V28, China). Mulberry fruit juice was filtered through a 120-mesh fine gauze and then centrifuged at 8,000 rpm for 20 min at 4 °C (Dynamica, Velocity 18R, United Kingdom). After centrifugation, the precipitate was discarded and the remainder was stored in a refrigerator at -80 °C for later use.

2.3. Synthesis of M-AgNPs

M-AgNPs were synthesized using a typical process described following. 4 mL of mulberry fruit juice and 2mL $AgNO_3$ (20 mM) were added into a centrifuge tube. Rapidly, the pH was adjusted to 10.0 using NaOH (1 M) solution. The mixed solution was put into an ultrasonic machine (Kunshan Ultrasonic, KQ-500DE, China) for the reaction using a power of 200 w at 60 °C for 2 h. At the end of the reaction, firstly the tube was centrifuged at 4°C and 5,000 rpm for 10 min, after which precipitates including the potential formed silver oxide (Ag_2O) were discarded. Further, the supernatant was centrifuged at 4 °C and 10,000 rpm for 10 min to isolate M-AgNPs, and then the newly obtained precipitates were resuspended in sterile ultrapure water to eliminate unreacted biomolecules. The process of centrifugation at 10,000 rpm and resuspension in ultrapure water was repeated thrice to ensure better purifying of M-AgNPs. Finally, M-AgNPs resuspended in sterile ultrapure water were vortexed and ultrasonicated for 20 min to obtain the M-AgNPs dispersion, which was then stored at 4 °C. On the other hand, the M-AgNPs powder was obtained by vacuum freeze-drying, which would be used for the further characterization experiments. This is only a typical example of the synthetic process, afterwards reaction parameters were optimized on this basis.

2.4. Optimization of reaction parameters

The antibacterial activity of AgNPs is closely related to the particle size, and the smaller particle size, the stronger antibacterial effect [7]. In order to obtain AgNPs with smaller particle size, key parameters in the synthesis process, including reaction time, temperature, pH, and $AgNO_3$ concentration, were ordinally optimized. Detailed experimental groups included reaction time (0.5, 1, 2, 3, 4 h), temperature (40, 50, 60, 70, 80 °C), pH (7.0, 8.0, 9.0, 10.0, 11.0), $AgNO_3$ concentration (10, 20, 40, 60, 80 mM). Initial experimental conditions of 60 °C, pH 10.0 and 20 mM $AgNO_3$ were used to optimize the reaction time. Based on a single-factor experiment, only the levels of one parameter were changed in each iteration. The level of parameter with the smaller particle size in each iteration was selected as the optimum condition and used in the next iteration. Three repeated samples were set for each level, and the results were expressed as "mean ± standard deviation".

2.5. Characterization of M-AgNPs

The formed silver nanomaterials were preliminarily characterized using ultraviolet-visible (UV-Vis) spectroscopy. A microplate reader (DeTie, HSB-ScanX, China) was used to record the surface plasmon resonance (SPR) absorption peaks of M-AgNPs in the wavelength range of 330-1000 nm. The X-ray diffraction (XRD) spectrum of M-AgNPs was analysed in the 2θ range (5-90 °) using an X-ray diffractometer (Bruker, D8 Advance, Germany), which was equipped with Cu-Kα radiation (λ = 1.54 Å). The surface functional groups of M-AgNPs were identified using a Fourier transform infrared (FI-IR) spectrometer (Shimadzu, IRAffinity-1S, Japan) in the range of 400~4000 cm^{-1}. Based on the dynamic light scattering (DLS), the particle size and Zeta potential of M-AgNPs were measured using a laser particle sizer (Malvern, Nano ZS90, United Kingdom). The morphology of M-AgNPs was observed using transmission electron microscopy (TEM) (JEOL, JEM 2100F, Japan) with an accelerating voltage of 200 kV.

2.6. Evaluation of antioxidant activity

The antioxidant activity of M-AgNPs was evaluated by the DPPH radical clearance rate, refer to the method of Sicari [24], with minor modifications. In 96-well microplates, each "test sample" was a

 doi:10.20944/preprints202311.0868.v1

mixture of 100 μL DPPH ethanol solution (0.1 mM) and 100 μL M-AgNPs dispersions with concentrations of 0.1, 0.2, 0.4, 0.8, and 1.6 mg/mL, respectively. The mixture including equal volume of anhydrous ethanol instead of DPPH ethanol solution was considered as the "background sample", whereas the mixture including equal volume of ultrapure water instead of M-AgNPs dispersion was considered as the "blank sample". 2, 6-Di-tert-butylp-cresol (BHT), a commonly used food antioxidant, was used as a positive control. Three replicates were set for each sample, and the results were expressed as "mean ± standard deviation". Their absorbance (λ = 517 nm) was measured after samples reacted in the dark for 30 min. The DPPH radical clearance rate was calculated according to the following formula:

$$\text{DPPH radical clearance activity (\%)} = [\, 1 - (A_1 - A_2) / A_0 \,] \times 100, \quad (1)$$

In this formula, A_1 is the absorbance of the test sample; A_2 is the absorbance of the background sample; A_0 is the absorbance of the blank sample.

2.7. Evaluation of antibacterial activity

The antibacterial activity of M-AgNPs against *S.aureus*, *E.coli* and *P.aeruginosa* was investigate by the "Oxford cup" method. Before the experiment, all containers and tools were sterilized at 121 °C for 30 min. Each agar plate was prepared using 20 mL of sterile LB medium. The three cryopreserved bacteria were scribed on agar plates, and then cultured at 37 °C for 24 h to activate them. The activated bacteria were prepared into bacterial suspensions (5×10^5 cfu/mL) using sterile saline. 200 μL of the bacterial suspensions was spread evenly on the agar plate, and then Oxford cups were placed smoothly on the surface. The 200 μL of M-AgNPs dispersion was injected into Oxford cups, and the same operation was performed with the same volume and concentration of C-AgNPs dispersion. After all samples were cultured at 37 °C for 24 h, the diameter of inhibition zone was measured by a vernier caliper. Three repeated samples were set for each drug of each bacterium, and the results were expressed as "mean ± standard deviation".

2.8. Statistical analysis

Statistical analyses were carried out using OriginPro software (Version 2023b, OriginLab Corporation, Northampton, MA, USA). One-way analysis of variance and Tukey's post hoc test were used to compare the differences between different groups. P value < 0.05 was considered statistically significant.

3. Results and Discussion

3.1. Synthesis of M-AgNPs and optimization of reaction parameters

3.1.1. The synthesis of silver nanoparticles

M-AgNPs were successfully synthesized by an environment-friendly method using mulberry fruit juice to reduce $AgNO_3$ solution. As shown in the illustration in Figure 1, the color of the mixed solution changed from brown (Figure 1a) to dark brown (Figure 1b), which suggested the formation of M-AgNPs. The active ingredients such as flavonoids, phenolic acids, terpenoids, alkaloids and reducing sugar in the mulberry fruit juice played roles of reducing agent and capping agent in the M-AgNPs forming process [15]. Figure 1 describes that the plant phenolic compounds reduced Ag ions and capped AgNPs. The two hydroxyl groups on the benzene ring lost H^+ and became O^-. O^- combined with Ag^+ through electrostatic interaction to form an intermediate silver complex. Further, when electrons were transferred to Ag^+, Ag ions were reduced to zero-valent silvers. Based on this interaction, polyphenol molecules formed a capping effect on silver atoms. As this reduction reaction continues, the crystal nucleus grew from the center to the periphery and eventually became M-AgNPs.

Preprints (www.preprints.org) | NOT PEER-REVIEWED | Posted: 14 November 2023 doi:10.20944/preprints202311.0868.v1

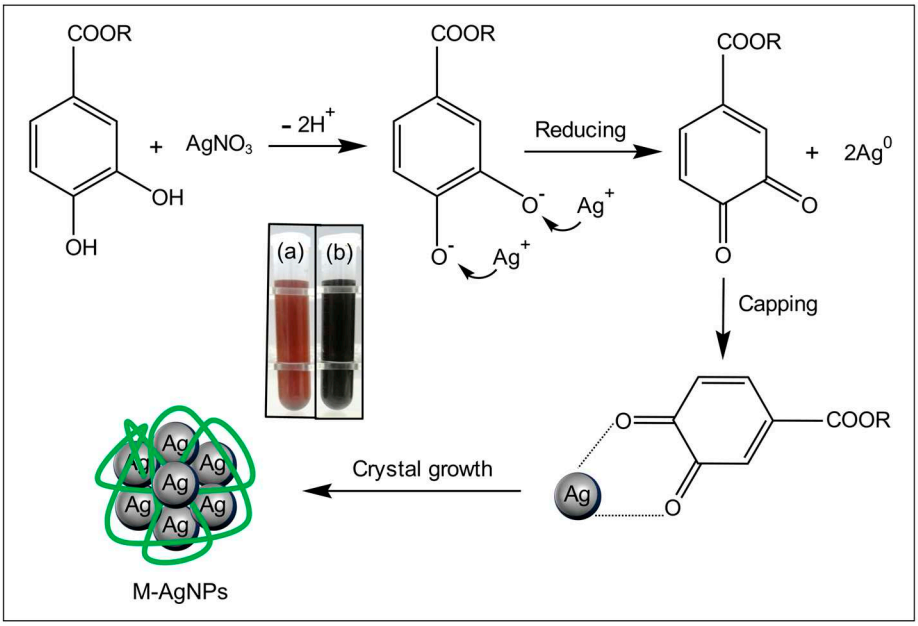

Figure 1. The mechanism of polyphenols reducing Ag ions and capping AgNPs [25]. (This image draws on Jagajjanani Rao's article and with minor modifications.).

3.1.2. Reaction time

To investigate the potential effect of the reaction time on the synthesizing M-AgNPs, the particle size of M-AgNPs was determined at five time points ranging from 0.5 h to 4 h. The results in Figure 2a show that the effect of reaction time on the particle size of M-AgNPs was not significant, which depended on continuous ultrasound. Some studies have shown that ultrasonic homogenization can prevent the agglomeration of silver nanoparticles [26,27]. Therefore, the particle size of M-AgNPs did not increase significantly with time when the mixed solution of mulberry fruit juice and $AgNO_3$ reacted in the ultrasonic machine. In order to pursue a simple process, the reaction time of 2h was chosen for the next iteration of the optimization experiment.

Preprints (www.preprints.org) | NOT PEER-REVIEWED | Posted: 14 November 2023 doi:10.20944/preprints202311.0868.v1

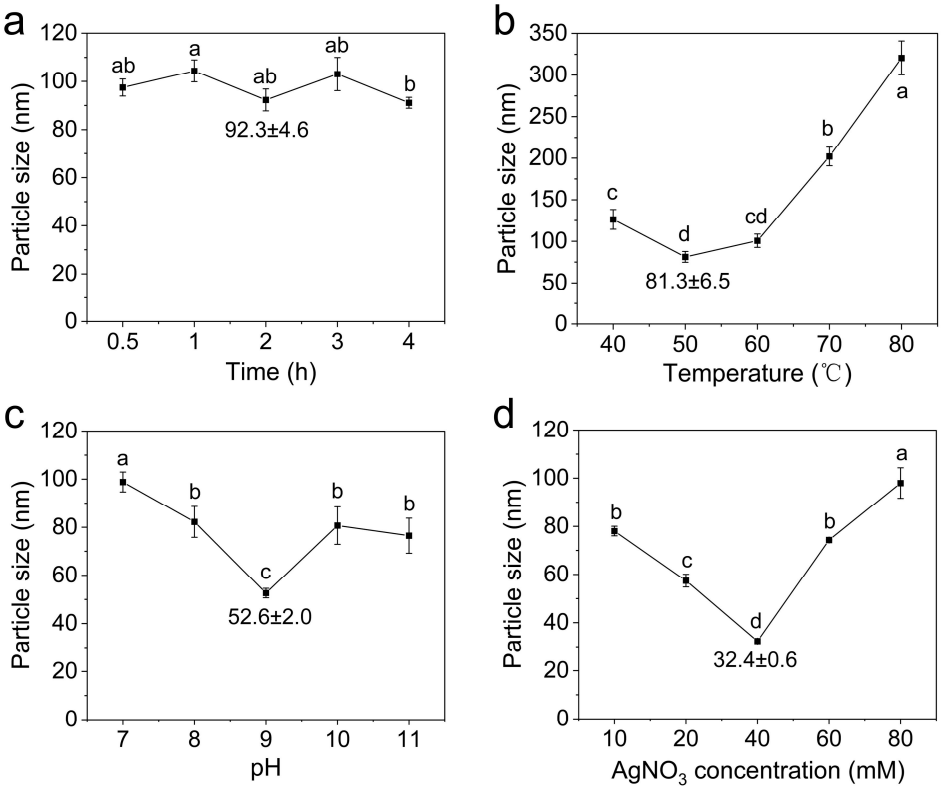

Figure 2. Optimization of reaction parameters: (a) reaction time, (b) temperature, (c) pH, (d) $AgNO_3$ concentration. There are significant differences between data points that do not share letters ($P < 0.05$). The detailed data are shown in Supplementary Table S1.

3.1.3. Reaction temperature

Most studies have shown that appropriate high temperature is favorable for the synthesis of AgNPs [28,29], because it can improve the reaction rate and obtain AgNPs with small particle size. However, a too high temperature may result in a greater particle size. As shown in Figure 2b, when the temperature exceeded 60 °C, the particle size increased sharply (> 100 nm). There are two reasons for this phenomenon: (i) The rapid growth of M-AgNPs crystal nucleus at high temperatures might lead to the formation of larger particles [30]; (ii) The active molecules covering on the surface of M-AgNPs were inactivated at high temperature, which led to the aggregation of AgNPs [31]. Therefore, for the smaller particle size and energy saving, 50 °C was chosen for the next iteration.

3.1.4. pH

The pH value was proved to affect the stability and capping ability of biomolecules by changing their electrical load, which directly influence the synthesis of AgNPs [32]. Most studies have shown that alkaline environment is more conducive to the synthesis of AgNPs than acidic environment [32–34]. Therefore, we further optimized the pH condition based on the above selected reaction time and temperature. As shown in Figure 2c, the particle size decreased gradually from pH 7.0 to pH 9.0. However, beyond pH 9.0, the particle size increased significantly. This phenomenon is attributed to the fact that a strongly alkaline pH potentially reduced the activity of plant molecules. Therefore, pH 9.0 was chosen for the further optimization.

3.1.5. Concentration of $AgNO_3$

Based on the conditions of reaction time of 2 h, 50 °C and pH 9.0, we further investigated the effects of $AgNO_3$ concentration on the synthesis of M-AgNPs. As shown in Figure 2d, the particle size of M-AgNPs decreased gradually with the increase of $AgNO_3$ concentration from 10mM to 40 mM.

Preprints (www.preprints.org) | NOT PEER-REVIEWED | Posted: 14 November 2023 doi:10.20944/preprints202311.0868.v1

However, the particle size suddenly increased when the $AgNO_3$ concentration reached 60 or 80 mM. This phenomenon may be due to the fact that the unreacted Ag ions enriched on the surface of the formed M-AgNPs, when the concentration of Ag ions was too high. The Ag ions enriching on the surface of M-AgNPs subsequently triggered a secondary reduction reaction, which led to the increase of particle size [35]. Therefore, 40 mM was used as the optimal concentration.

3.2. Characterization of M-AgNPs

3.2.1. UV-Vis absorption spectrum

Due to the surface plasmon resonance (SPR) of nano-metal particles, silver nanoparticles appear SPR characteristic absorption peaks among 350~500 nm spectrum range [12]. Based on this optical principle, the formation of AgNPs can be confirmed. In our study, M-AgNPs synthesized using mulberry fruit juice exhibited a SPR characteristic absorption peak at 434 nm (Figure 3a), which was caused by the color change of the mixed solution mentioned above. As negative controls, there were no absorption peak in the mulberry fruit juice and $AgNO_3$ solution.

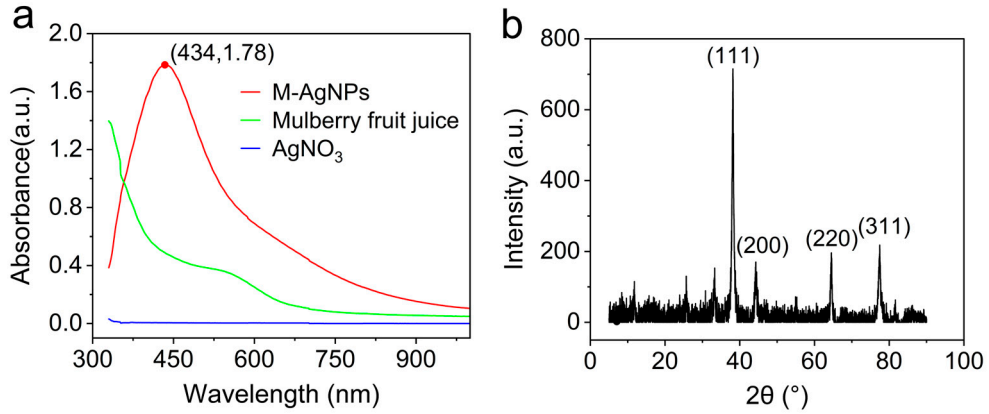

Figure 3. (a) UV-Vis spectrum of M-AgNPs, mulberry fruit juice and $AgNO_3$ solution, (b) XRD spectrum of M-AgNPs.

3.2.2. XRD absorption spectrum

X-ray diffraction (XRD) technique is often used for phase characterization and crystal structure analysis of samples. Figure 3b shows the XRD spectrogram of the synthesized M-AgNPs. The diffraction peaks at 2θ values of 38.16°, 44.30°, 64.52° and 77.48° represented the (111), (200), (220) and (311) Bragg reflections, respectively. According to JCPDS card No. 87-0720, the observed diffraction peaks indicated the face centered cubic (fcc) structure of Ag, which were similar to silver nanoparticles synthesized using other plants [34,36].

3.2.3. FT-IR absorption spectrum

The biological molecules reducing Ag^+ and capping AgNPs were analyzed by Fourier transform infrared absorption spectrum (FT-IR). The mulberry fruit juice and M-AgNPs synthesized using the mulberry fruit juice appeared many similar absorption peaks (Figure 4). The several absorption peaks around 1540 cm^{-1} were caused by the C=C stretching vibration of the benzene ring skeleton, which indicated that aromatic compounds existed on the surface of M-AgNPs [37]. On this basis, the presence of polyphenols was confirmed by C-O stretching vibrations at 1096 cm^{-1} and hydroxyl (-OH) stretching vibrations at 3396 cm^{-1}. The absorption peak at 1653 cm^{-1} might be caused by the carbonyl group (C=O) on the flavone. The two absorption peaks at 2849, 2919 cm^{-1} might be generated by C-H stretching of alkanes, aldehyses, or aromatic hydrocarbons, which was observed in previous report [38]. All of these suggested that phenols, flavonoids and other metabolites in mulberry fruit juice are major players in reducing Ag^+ and capping AgNPs.

Preprints (www.preprints.org) | NOT PEER-REVIEWED | Posted: 14 November 2023 doi:10.20944/preprints202311.0868.v1

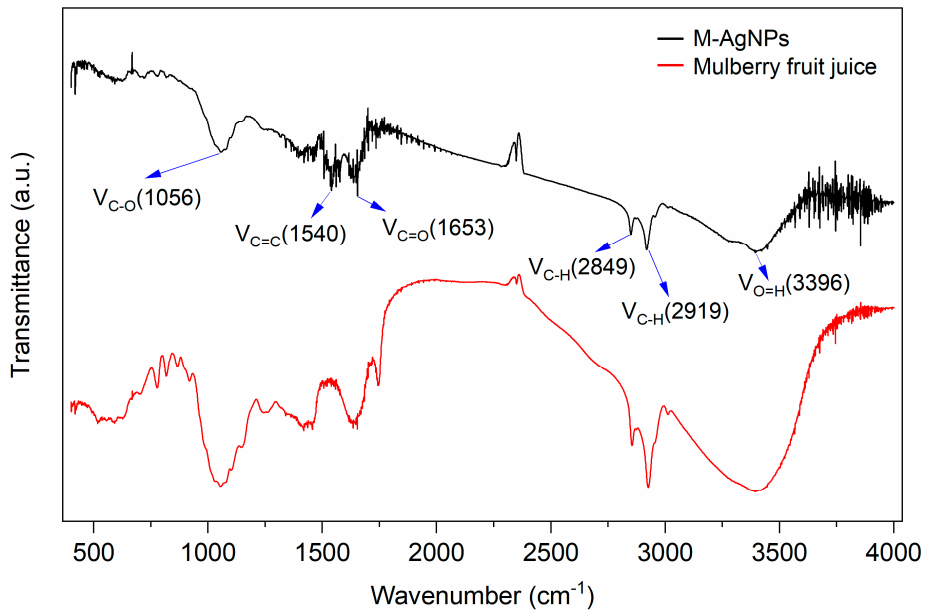

Figure 4. FT-IR spectrum of M-AgNPs and mulberry fruit juice.

3.2.4. DLS analysis

The particle size distribution and Zeta potential of M-AgNPs dispersion were analyzed by dynamic light scattering (DLS). As shown in Figure 5a, the size of M-AgNPs were concentrated within 100 nm and their average particle size was 32.7 nm. In Figure 5c, the average Zeta potential value of M-AgNPs was -23.3 mV, which is close to that reported previously [3,36]. The negative potential value guaranteed the stability of M-AgNPs, which was due to the adsorption of biological molecules on its surface. As shown in Figure 5b, d, the particle size and Zeta potential values of M-AgNPs did not change greatly within 60 days, which indicated that the nanosilver synthesized using mulberry fruit juice has well stability.

Preprints (www.preprints.org) | NOT PEER-REVIEWED | Posted: 14 November 2023 doi:10.20944/preprints202311.0868.v1

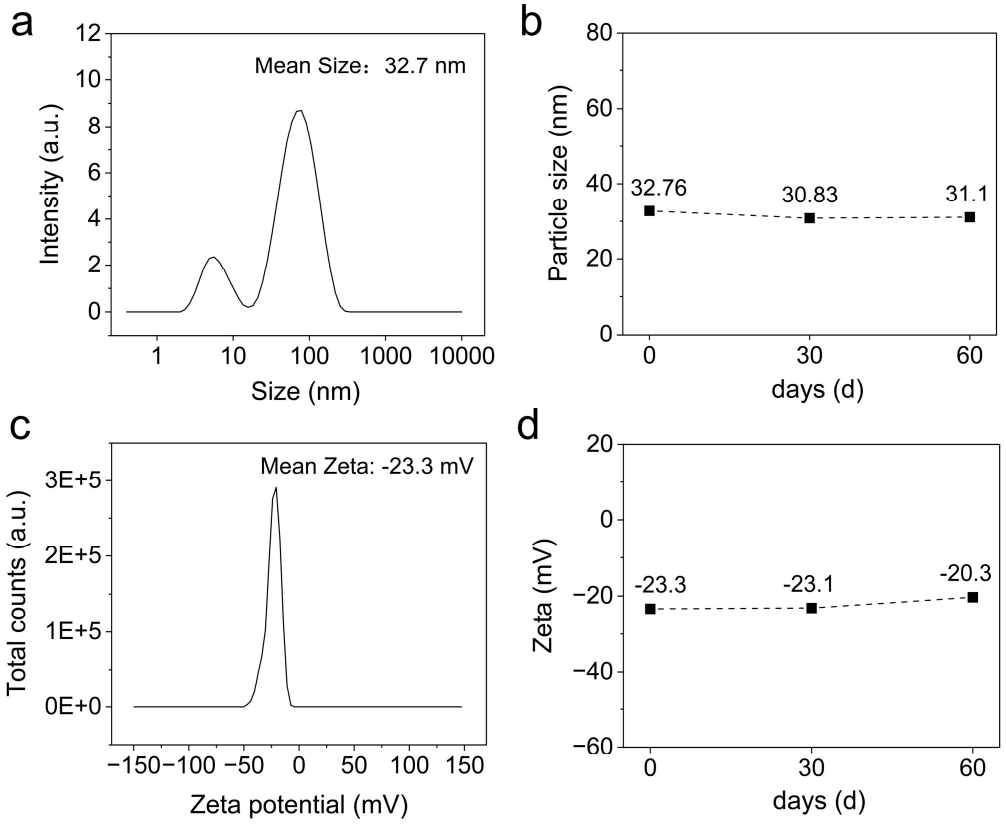

Figure 5. Particle size (a) and Zeta potential (c) distribution of M-AgNPs. M-AgNPs' stability was evaluated by measuring the particle size (b) and Zeta potential (d) at 0, 30 and 60 days, respectively.

3.2.5. TEM observation

The morphology of M-AgNPs was observed by transmission electron microscopy (TEM). As shown in Figure 6a, most of the M-AgNPs were approximately spherical, with good dispersibility. The sizes of the particles in the TEM images were counted. The frequency distribution histogram of particle size (Figure 6b) shows that M-AgNPs were between 18.9 nm and 37.7 nm, with an average particle size of 28.7 nm, which was slightly smaller than the data of DLS analysis. Similar data differences also appeared in other studies [3]. The potential reason for this difference is that the hydration layer of the test solution caused the larger particle size of M-AgNPs for DLS analysis.

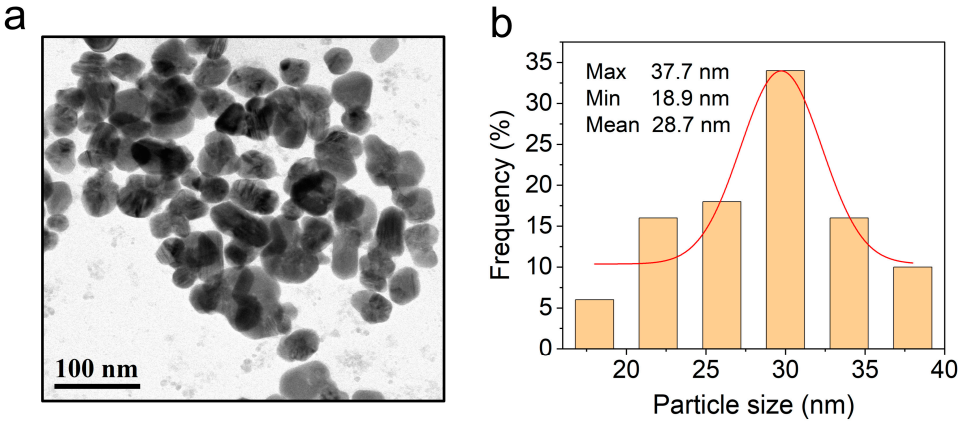

Figure 6. TEM images and particle size's frequency distribution histogram of M-AgNPs.

Preprints (www.preprints.org) | NOT PEER-REVIEWED | Posted: 14 November 2023 doi:10.20944/preprints202311.0868.v1

3.3. Antioxidant activity of M-AgNPs

1,1-Diphenyl-2-trinitrophenylhydrazine (DPPH), a stable radical, can be reduced by accepting hydrogen or electrons provided by antioxidants. When radical scavengers are added, the color change of DPPH solution is linearly related to the decreased level of absorbance [39]. Therefore, DPPH radical clearance rate was used to evaluate the antioxidant ability of a given sample. As shown in Figure 7, the DPPH radical clearance rate of M-AgNPs increased in a dose-dependent manner. On the other hand, in the range of 0.1 to 1.6 mg/mL, the clearance ability of BHT did not significantly change. Although at lower concentrations (0.1~0.4 mg/mL), the clearance ability of M-AgNPs was less potent than BHT. However, the clearance ability of M-AgNPs (79.47%) was better than that of BHT (69.87%) at 1.6 mg/mL. More details of the data are available in Supplementary Table S2. The antioxidant activity of M-AgNPs is attributed to active molecules attached to their surface [39]. It is well known that phenols and flavonoids in plants are good natural antioxidants [40].

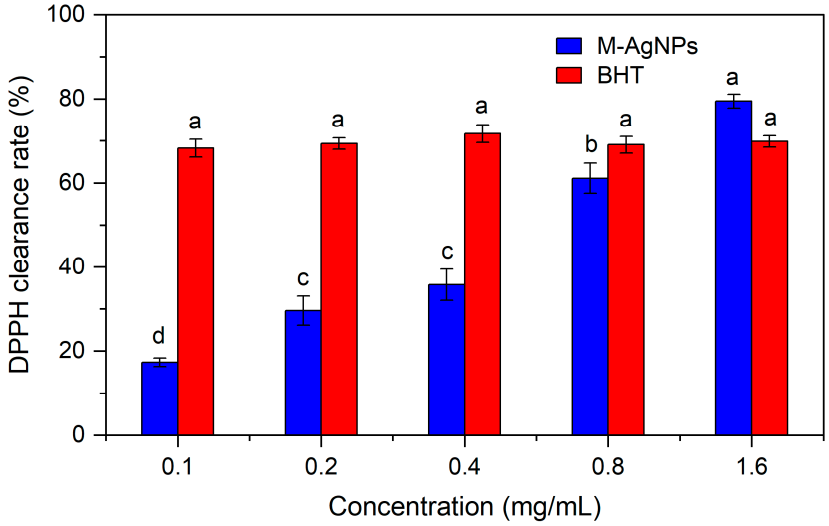

Figure 7. DPPH radical clearance rate of M-AgNPs and BHT. In different concentrations of an antioxidant, data that do not share letters represents significant differences ($P < 0.05$). The detailed data are provided in Supplementary Table S2.

3.4. Antibacterial activity of M-AgNPs

After the bacteria were cultured for 24 h, the diameters of inhibition zone (DIZs) of two kinds of silver nanoparticles against *P.aeruginosa*, *E.coli* and *S.aureus* were measured (Figure 8b). The DIZs of M-AgNP against the above three bacteria were 13.9 ± 0.4, 12.2 ± 0.3, and 12.8 ± 0.7 mm, respectively, whereas the DIZs of C-AgNPs were 11.0 ± 0.8, 9.8 ± 0.1, and 10.5 ± 0.9 mm, respectively. Figure 8a shows that the DIZs of M-AgNPs were significantly larger than those of C-AgNPs. It is reported that flavonoids in mulberry fruit have inhibitory effects on *E. coli* and *S.aureus* [15]. Mulberry fruit anthocyanins can also interfere with bacterial metabolism by inhibiting the activity of enzymes relating to growth [41]. Together with our results, it is indicated that the enhanced antibacterial effects of M-AgNPs might attribute to the mulberry fruit's active molecules attached on M-AgNPs.

Preprints (www.preprints.org) | NOT PEER-REVIEWED | Posted: 14 November 2023 doi:10.20944/preprints202311.0868.v1

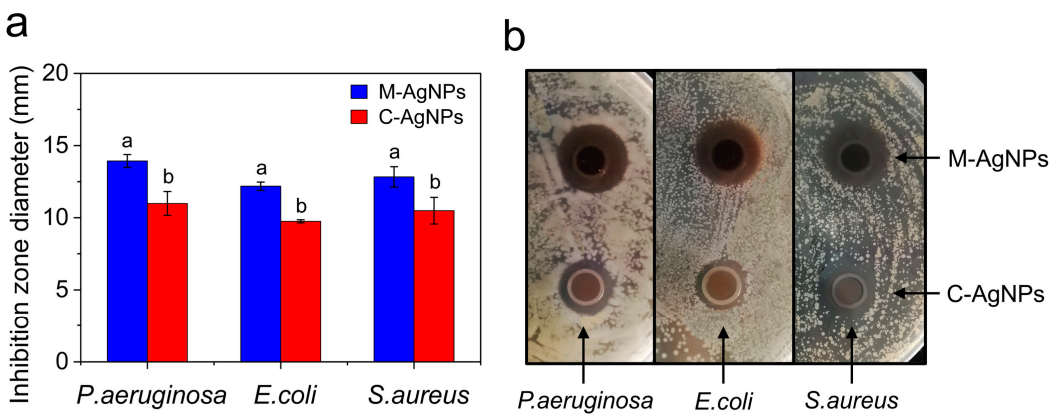

Figure 8. The inhibition zone of M-AgNPs and C-AgNPs. For the same bacterium, the two groups that do not share letters have significant differences ($P < 0.05$).

As mentioned above, the antibacterial mechanism of AgNPs is multi-way, therefore it has no bacterial resistance. Figure 9 shows the antibacterial mechanism of M-AgNPs. The antibacterial mechanism of silver nanoparticles mainly includes: (i) cell wall and cell membrane damage, (ii) intracellular functional damage, (iii) oxidative stress [7]. M-AgNPs first adhere to the microbial cell wall and membrane through electrostatic interactions, which changes the permeability of cell membrane [42]. Subsequently, M-AgNPs release Ag ions that penetrate the cell wall and enter the cell, causing a series of intracellular injuries. Ag ions cause functional protein denaturation and enzyme inactivation by binding to sulfur-containing proteins [43]. In addition, Ag ions can also affect ribosomal subunits, leading to the termination of protein synthesis [42]. More importantly, Ag ions induces intracellular oxidative stress, and a large amount of reactive oxygen species (ROS) is released. Excessive ROS can lead to a range of malignant events, such as DNA damage, respiratory chain function destruction, and ultimately bacterial death [44,45].

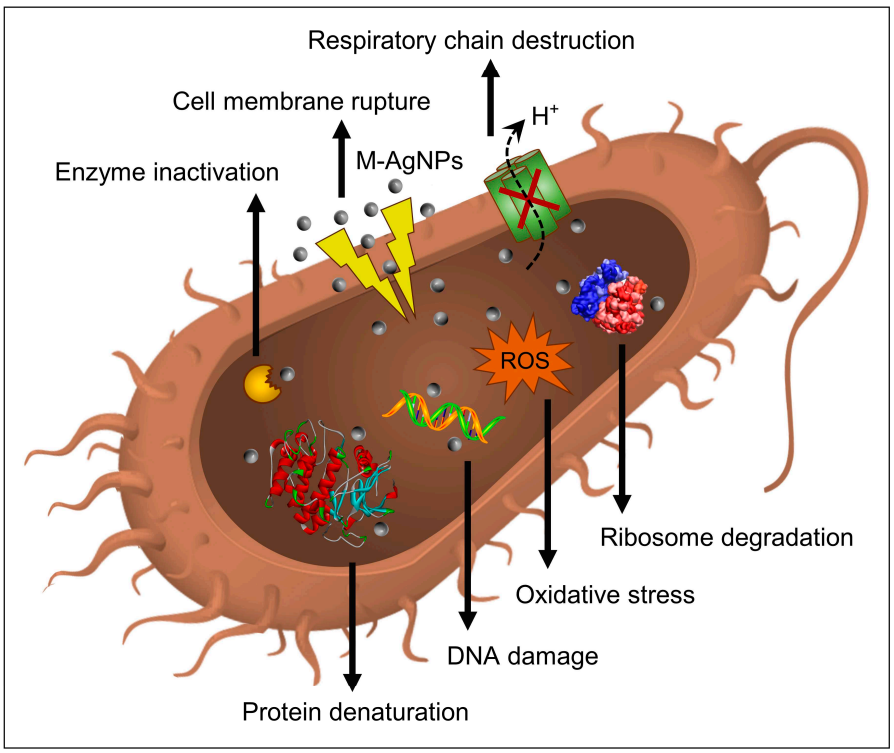

Figure 9. Sterilization mechanism of AgNPs. (The bacterial model is from "Vecteezy.com".).

4. Conclusions

M-AgNPs, a composite nanomaterial encapsulated by bioactive components, have been successfully synthesized using an environmentally friendly process. The key parameters of synthesis process including reaction time, temperature, pH value, $AgNO_3$ concentration were optimized to prepare M-AgNPs with a minimum particle size of about 30 nm. UV-Vis and XRD revealed the formation of M-AgNPs with face centered cubic structure. FT-IR confirmed the reducting and capping effect of active ingredients in mulberry fruits (flavonoids, phenolic acids, etc.) on M-AgNPs. Approximately spherical and equably distributed M-AgNPs were observed by TEM. The antioxidant activity of mulberry fruit polyphenols endowed M-AgNPs with a well DPPH radical clearance ability. AgNPs showed antibacterial activity against *P.aeruginosa*, *E.coli* and *S.aureus*. Due to the attachment of active molecules on its surface, the greenly synthesized M-AgNPs had better antibacterial activity than the chemically synthesized C-AgNPs. Our research has positive implications for the green synthesis of silver nanoparticles and their future applications. Furthermore, this research provides an interesting idea for the development of medicinal resource *Fructus mori*. In the future research, we will explore the detailed antibacterial mechanisms of M-AgNPs and the toxicity to normal cells.

Supplementary Materials: The following supporting information can be downloaded at the website of this paper posted on Preprints.org. Table S1: DPPH radical clearance rate of M-AgNPs and BHT; Table S2: Particle size of optimized parameters.

Author Contributions: Conceptualization, Jisheng Li and Wei Fan; Data curation, Fangzheng Liu and Wei Fan; Formal analysis, Na Li, Xiaoxuan Liu and Xiaoqing Jie; Investigation, Fangzheng Liu, Binbin Wang, Manli Jia and Yongxue Song; Methodology, Jisheng Li and Wei Fan; Project administration, Jisheng Li; Supervision, Jisheng Li; Validation, Fangzheng Liu, Binbin Wang, Manli Jia and Yongxue Song; Visualization, Na Li, Xiaoxuan Liu and Xiaoqing Jie; Writing – original draft, Fangzheng Liu; Writing – review & editing, Jisheng Li and Chuanjing An. All authors have read and agreed to the published version of the manuscript.

Funding: This work was supported by the Funding Project of Hebei Provincial Education Department for Graduate Innovation Ability Training (CXZZSS2023139) and Key R & D Projects of Hebei Province (20326336D).

Data Availability Statement: Not applicable.

Conflicts of Interest: All authors declare that there is no conflict of interest.

References

1. Parashar, S.; Sharma, M.K.; Garg, C.; Garg, M. Green synthesized silver nanoparticles as silver lining in antimicrobial resistance: A review. *Curr. Drug Delivery* **2022**, *19*, 170-181. [CrossRef]
2. Huq, M.A.; Ashrafudoulla, M.; Rahman, M.M.; Balusamy, S.R.; Akter, S. Green synthesis and potential antibacterial applications of bioactive silver nanoparticles: A review. *Polymers* **2022**, *14*, 742. [CrossRef]
3. Khane, Y.; Benouis, K.; Albukhaty, S.; Sulaiman, G.M.; Abomughaid, M.M.; Al Ali, A.; Aouf, D.; Fenniche, F.; Khane, S.; Chaibi, W., *et al.* Green synthesis of silver nanoparticles using aqueous citrus limon zest extract: Characterization and evaluation of their antioxidant and antimicrobial properties. *Nanomaterials* **2022**, *12*, 2013. [CrossRef]
4. ElNaggar, N.E.; Hussein, M.H.; ElSawah, A.A. Bio-fabrication of silver nanoparticles by phycocyanin, characterization, in vitro anticancer activity against breast cancer cell line and in vivo cytotxicity. *Sci. Rep.* **2017**, *7*. [CrossRef]
5. Velmurugan, P.; Anbalagan, K.; Manosathyadevan, M.; Lee, K.; Cho, M.; Lee, S.; Park, J.; Oh, S.; Bang, K.; Oh, B. Green synthesis of silver and gold nanoparticles using zingiber officinale root extract and antibacterial activity of silver nanoparticles against food pathogens. *Bioprocess Biosyst. Eng.* **2014**, *37*, 1935-1943. [CrossRef]
6. Wang, L.; Hu, C.; Shao, L. The antimicrobial activity of nanoparticles: Present situation and prospects for the future. *Int. J. Nanomed.* **2017**, *12*, 1227-1249. [CrossRef]
7. Roy, A.; Bulut, O.; Some, S.; Mandal, A.K.; Yilmaz, M.D.; Roy, A. Green synthesis of silver nanoparticles: Biomolecule-nanoparticle organizations targeting antimicrobial activity. *RSC Adv.* **2019**, *9*, 2673-2702. [CrossRef]

8. Khatoon, U.T.; Rao, G.V.S.N.; Mantravadi, K.M.; Oztekin, Y. Strategies to synthesize various nanostructures of silver and their applications – a review. *RSC Adv.* **2018**, *8*, 19739-19753. [CrossRef]
9. Nguyen, D.D.; Lai, J.Y. Synthesis, bioactive properties, and biomedical applications of intrinsically therapeutic nanoparticles for disease treatment. *Chem. Eng. J.* **2022**, *435*, 134970. [CrossRef]
10. Rafique, M.; Sadaf, I.; Rafique, M.S.; Tahir, M.B. A review on green synthesis of silver nanoparticles and their applications. *Artif. Cells, Nanomed., Biotechnol.* **2016**, *45*, 1272-1291. [CrossRef]
11. Mustapha, T.; Misni, N.; Ithnin, N.R.; Daskum, A.M.; Unyah, N.Z. A review on plants and microorganisms mediated synthesis of silver nanoparticles, role of plants metabolites and applications. *Int. J. Environ. Res. Public Health* **2022**, *19*, 674. [CrossRef]
12. Ahmad, B.; Shireen, F.; Rauf, A.; Shariati, M.A.; Bashir, S.; Patel, S.; Khan, A.; Rebezov, M.; Khan, M.U.; Mubarak, M.S., *et al.* Phyto-fabrication, purification, characterisation, optimisation, and biological competence of nano-silver. *IET Nanobiotechnol.* **2021**, *15*, 1-18. [CrossRef]
13. Habeeb Rahuman, H.B.; Dhandapani, R.; Narayanan, S.; Palanivel, V.; Paramasivam, R.; Subbarayalu, R.; Thangavelu, S.; Muthupandian, S. Medicinal plants mediated the green synthesis of silver nanoparticles and their biomedical applications. *IET Nanobiotechnol.* **2022**, *16*, 115-144. [CrossRef]
14. Chen, T.; Shuang, F.; Fu, Q.; Ju, Y.; Zong, C.; Zhao, W.; Zhang, D.; Yao, X.; Cao, F. Evaluation of the chemical composition and antioxidant activity of mulberry (*morus alba l.*) fruits from different varieties in china. *Molecules* **2022**, *27*, 2688. [CrossRef]
15. Hao, J.; Gao, Y.; Xue, J.; Yang, Y.; Yin, J.; Wu, T.; Zhang, M. Phytochemicals, pharmacological effects and molecular mechanisms of mulberry. *Foods* **2022**, *11*, 1170. [CrossRef]
16. Jin, Q.; Yang, J.; Ma, L.; Wen, D.; Chen, F.; Li, J. Identification of polyphenols in mulberry (*genus morus*) cultivars by liquid chromatography with time-of-flight mass spectrometer. *J. Food Compos. Anal.* **2017**, *63*, 55-64. [CrossRef]
17. Paunović, S.M.; Mašković, P.; Milinković, M. Determination of primary metabolites, vitamins and minerals in black mulberry (morus nigra) berries depending on altitude. *Erwerbs-Obstbau* **2020**, *62*, 355-360. [CrossRef]
18. Bhattacharjya, D.; Sadat, A.; Dam, P.; Buccini, D.F.; Mondal, R.; Biswas, T.; Biswas, K.; Sarkar, H.; Bhuimali, A.; Kati, A., *et al.* Current concepts and prospects of mulberry fruits for nutraceutical and medicinal benefits. *Curr. Opin. Food Sci.* **2021**, *40*, 121-135. [CrossRef]
19. Chen, C.; You, L.; Abbasi, A.M.; Fu, X.; Liu, R.H. Optimization for ultrasound extraction of polysaccharides from mulberry fruits with antioxidant and hyperglycemic activity in vitro. *Carbohydr. Polym.* **2015**, *130*, 122-132. [CrossRef]
20. Cheng, K.; Wang, C.; Chang, Y.; Hung, T.; Lai, C.; Kuo, C.; Huang, H. Mulberry fruits extracts induce apoptosis and autophagy of liver cancer cell and prevent hepatocarcinogenesis in vivo. *J. Food Drug Anal.* **2020**, *28*, 84-93. [CrossRef]
21. Jiang, Y.; Dai, M.; Nie, W.; Yang, X.; Zeng, X. Effects of the ethanol extract of black mulberry (*morus nigra l.*) fruit on experimental atherosclerosis in rats. *J. Ethnopharmacol.* **2017**, *200*, 228-235. [CrossRef]
22. Li, Y.; Bao, T.; Chen, W. Comparison of the protective effect of black and white mulberry against ethyl carbamate-induced cytotoxicity and oxidative damage. *Food Chem.* **2018**, *243*, 65-73. [CrossRef]
23. Jia, M.; Li, N.; Wang, B.; Fan, W.; Xia, A.; Li, J. Evaluation of nutrition, aroma components and antioxidant activity ofmulberry fruits from nine varieties. *J. Fruit Sci* **2022**, *39*, 221-232. [CrossRef]
24. Sicari, V.; Loizzo, M.R.; Branca, V.; Pellicanò, T.M. Bioactive and antioxidant activity from citrus bergamia risso (*bergamot*) juice collected in different areas of reggio calabria province, italy. *Int. J. Food Prop.* **2016**, *19*, 1962-1971. [CrossRef]
25. Jagajjanani Rao, K.; Paria, S. Green synthesis of silver nanoparticles from aqueous aegle marmelos leaf extract. *Mater. Res. Bull.* **2013**, *48*, 628-634. [CrossRef]
26. Barbhuiya, R.I.; Singha, P.; Asaithambi, N.; Singh, S.K. Ultrasound-assisted rapid biological synthesis and characterization of silver nanoparticles using pomelo peel waste. *Food Chem.* **2022**, *385*, 132602. [CrossRef]
27. Gevorgyan, S.; Schubert, R.; Yeranosyan, M.; Gabrielyan, L.; Trchounian, A.; Lorenzen, K.; Trchounian, K. Antibacterial activity of royal jelly-mediated green synthesized silver nanoparticles. *AMB Express* **2021**, *11*. [CrossRef]
28. Li, Z.; Ma, W.; Ali, I.; Zhao, H.; Wang, D.; Qiu, J. Green and facile synthesis and antioxidant and antibacterial evaluation of dietary myricetin-mediated silver nanoparticles. *ACS Omega* **2020**, *5*, 32632-32640. [CrossRef]

29. Muniyappan, N.; Nagarajan, N.S. Green synthesis of silver nanoparticles with dalbergia spinosa leaves and their applications in biological and catalytic activities. *Process Biochem.* **2014**, *49*, 1054-1061. [CrossRef]
30. Dong, C.F.; Cheng, F.; Zhang, X.L.; Wang, X.J.; Yang, X.Z.; Yuan, B. Rapid and green synthesis of monodisperse silver nanoparticles using mulberry leaf extract. *Rare Metal Mat. Eng.* **2018**, *47*, 1089-1095. [CrossRef]
31. Manjari Mishra, P.; Kumar Sahoo, S.; Kumar Naik, G.; Parida, K. Biomimetic synthesis, characterization and mechanism of formation of stable silver nanoparticles using *averrhoa carambola l.* Leaf extract. *Mater. Lett.* **2015**, *160*, 566-571. [CrossRef]
32. Lade, B.D.; Shanware, A.S. Phytonanofabrication: Methodology and factors affecting biosynthesis of nanoparticles. *Smart Nanosyst. Biomed., Optoelectron. Catal.* **2020,** 6. [CrossRef]
33. Jain, S.; Mehata, M.S. Medicinal plant leaf extract and pure flavonoid mediated green synthesis of silver nanoparticles and their enhanced antibacterial property. *Sci. Rep.* **2017**, *7*. [CrossRef]
34. Nouri, A.; Tavakkoli Yaraki, M.; Lajevardi, A.; Rezaei, Z.; Ghorbanpour, M.; Tanzifi, M. Ultrasonic-assisted green synthesis of silver nanoparticles using *mentha aquatica* leaf extract for enhanced antibacterial properties and catalytic activity. *Colloid Interface Sci. Commun.* **2020**, *35*, 100252. [CrossRef]
35. Yang, N.; Hao, L.; Yang, P. Mango peel extract mediated novel route for synthesis of silver nanoparticles and antibacterial application of silver nanoparticles. *J. Shanxi Agr. Uni.* **2013**, *33*, 59-65. [CrossRef]
36. Chandraker, S.K.; Lal, M.; Khanam, F.; Dhruve, P.; Singh, R.P.; Shukla, R. Therapeutic potential of biogenic and optimized silver nanoparticles using rubia cordifolia l. Leaf extract. *Sci. Rep.* **2022**, *12*. [CrossRef]
37. Sathiya, C.K.; Akilandeswari, S. Fabrication and characterization of silver nanoparticles using delonix elata leaf broth. *Spectrochim. Acta, Part A* **2014**, *128*, 337-341. [CrossRef]
38. Zia, M.; Gul, S.; Akhtar, J.; Ul Haq, I.; Abbasi, B.H.; Hussain, A.; Naz, S.; Chaudhary, M.F. Green synthesis of silver nanoparticles from grape and tomato juices and evaluation of biological activities. *IET Nanobiotechnol.* **2017**, *11*, 193-199. [CrossRef]
39. Bhakya, S.; Muthukrishnan, S.; Sukumaran, M.; Muthukumar, M. Biogenic synthesis of silver nanoparticles and their antioxidant and antibacterial activity. *Applied Nanoscience* **2015**, *6*, 755-766. [CrossRef]
40. Khoshnamvand, M.; Huo, C.; Liu, J. Silver nanoparticles synthesized using allium ampeloprasum l. Leaf extract: Characterization and performance in catalytic reduction of 4-nitrophenol and antioxidant activity. *J. Mol. Struct.* **2019**, *1175*, 90-96. [CrossRef]
41. Kim, B.S.; Kim, H.; Kang, S.-S. In vitro anti-bacterial and anti-inflammatory activities of lactic acid bacteria-biotransformed mulberry (*morus alba linnaeus*) fruit extract against salmonella typhimurium. *Food Control* **2019**, *106*, 106758. [CrossRef]
42. Dakal, T.C.; Kumar, A.; Majumdar, R.S.; Yadav, V. Mechanistic basis of antimicrobial actions of silver nanoparticles. *Front Microbiol.* **2016**, *7*, 1831. [CrossRef]
43. Wigginton, N.S.; Titta, A.d.; Piccapietra, F.; Dobias, J.; Nesatyy, V.J.; Suter, M.J.F.; Bernier-Latmani, R. Binding of silver nanoparticles to bacterial proteins depends on surface modifications and inhibits enzymatic activity. *Environ. Sci. Technol.* **2010**, *44*, 2163-2168. [CrossRef]
44. Belluco, S.; Losasso, C.; Patuzzi, I.; Rigo, L.; Conficoni, D.; Gallocchio, F.; Cibin, V.; Catellani, P.; Segato, S.; Ricci, A. Silver as antibacterial toward listeria monocytogenes. *Front Microbiol.* **2016**, *7*, 307. [CrossRef]
45. Slavin, Y.N.; Asnis, J.; Häfeli, U.O.; Bach, H. Metal nanoparticles: Understanding the mechanisms behind antibacterial activity. *J. Nanobiotechnol.* **2017**, *15*, 1-20. [CrossRef]